Journal of Materials Processing Tech. 291 (2021) 117040

Contents lists available at ScienceDirect

Journal of Materials Processing Tech.

journal homepage: www.elsevier.com/locate/jmatprotec

Penetration and mixing of filler wire in hybrid laser welding

W. Suder [a,*], S. Ganguly [a], S. Williams [a], B.Y.B. Yudodibroto [b]

[a] Welding Engineering and Laser Processing Centre, Cranfield University, MK43 0AL, Great Britain, United Kingdom
[b] Independent Researcher (Formerly With Heerema Marine Contractors), 2716PZ, the Netherlands

ARTICLE INFO

Associate Editor: Guest Editor (Exeter)

Keywords:
Hybrid laser welding
Wire mixing
Weld homogeneity
Productivity limit

ABSTRACT

Modern lasers allow achievement of full penetration single pass welds in steel plates with thicknesses exceeding 20 mm, at welding speeds much greater than any traditional arc-based process. However, the addition of filler wire, which in most structural welds is required to ensure good mechanical properties, is more challenging. Most welds from laser and hybrid welding with filler feeding start to exhibit inhomogeneous fusion zones above a particular joint thickness. The filler consumable segregates near the top section of the joint, while the bottom forms by the re-melted parent metal, which negatively affects mechanical properties. In this work, the homogeneity of laser-arc hybrid welds was investigated experimentally, using a filler wire with a signature element, whose distribution was measured. Three different bevels with different geometry were used to study the flow of liquid filler wire across the joint. The laser and arc parameters were varied to establish the dominant forces responsible for the transport of filler wire and weld homogeneity. The results indicate that hybrid welds are susceptible to form inhomogeneous fusion zones and to achieve acceptable welds, two aspects need to be controlled. The first one is the average content of an alloying element in the meltpool, which is mainly controlled by the wire composition, its deposition rate and dilution with the parent metal. Whilst the second aspect being the weld homogeneity. It has been found that the laser power density is predominantly responsible for the transport of the consumable metal across the material. Furthermore, most processing parameters, such as the arc power or laser power, play contradicting roles, improving one aspect and simultaneously hindering another. The best way of achieving fully homogenous welds with known composition is by applying sufficient wire deposition, to satisfy the compositional requirement, and then provide enough laser power density to transport it across the full thickness.

1. Introduction

Laser-arc hybrid welding utilises complementary benefits of laser and arc, namely the laser provides deep penetration and the arc source melts the filler consumable and enhances the weld profile. Therefore, the hybrid process offers better weld quality than the laser welding and greater productivity than any arc-based welding. However, the process stability and metallurgical aspects also have to be considered. At a certain point, the productivity is not limited by the available laser power but rather by the quality requirements. Sokolov et al. (2011) reported results on hybrid laser welding using a 30 kW fibre laser and found that it was challenging to penetrate more than 25 mm steel in a single pass due to the occurrence of defects. Hybrid laser welding is a relatively complex process. The keyhole stability, weld profile and microstructure are determined by the complex balance of different forces, such as vaporisation pressure, surface tension-driven convection, droplets momentum and the electromagnetic pressure of arc (Zhou and Tsai, 2008). The effect of welding parameters on most of these aspects has been understood by using numerical modelling and experimental investigations, however, what is the practical limit of penetration depth and productivity it is still an open question. Semak and Matsunawa (1997) pioneered the application of vapour recoil pressure acting on the liquid metal as the main driving force for the keyhole depth. In their model, the penetration depth was directly dependent on the vapour pressure, controlled by the laser intensity. Courtois et al. (2013) showed that the keyhole shape and its stability are additionally affected by the multi-reflections of the laser beam. The results revealed that the keyhole surface might undergo strong instabilities leading to its collapse. Many authors postulated that liquid-vapour interaction and stability of the keyhole ultimately limit the penetration depth. The vapour pressure has to continuously act against the surface tension of the liquid metal, which may lead to periodic oscillations, as recorded by Semak et al. (1995). It

* Corresponding author.
E-mail address: w.j.suder@cranfield.ac.uk (W. Suder).

https://doi.org/10.1016/j.jmatprotec.2020.117040
Received 8 October 2020; Received in revised form 22 December 2020; Accepted 29 December 2020
Available online 5 January 2021

has been even demonstrated theoretically that at certain frequencies of meltpool oscillation the keyhole may completely collapse (Klein et al., 1996). In a recent work, Zhang et al. (2019) developed a numerical model to study the dynamic behaviour of the keyhole and found that above a certain depth to width ratio, the keyhole becomes unstable and collapses. The mechanism of keyhole collapse defects has been demonstrated experimentally using X-ray imaging (Zhang et al., 2013) and numerically (Lu et al., 2015). Therefore despite the availability of high power lasers with output powers exceeding 50 kW in continuous wave mode, poor stability of the keyhole, when a certain depth to width ratio is reached, limits the maximum penetration depth that can be achieved in practice.

In structural welds, the limit of maximum thickness that can be welded is additionally limited by the weld homogeneity. For every combination of welding conditions, there is a maximum thickness of the workpiece, above which the weld profile of a hybrid weld separates into two distinguishable zones, i.e. arc-zone at the top and laser-zone in the deeper region (Hayashi et al., 2004). In such a case, it is very likely that the majority of filler wire is deposited in the arc-zone and the laser zone is mainly formed from the solidified parent metal, which in some cases is evident as a gradient of microstructure and mechanical properties of the joint (Mazar Atabaki et al., 2014). Inhomogeneous welds may lead to susceptibility to cracking in certain materials (Kujanpää, 2014). Therefore, the distribution of filler wire in a joint should be one of the main factors determining the practical limit of productivity, i.e. a maximum material thickness that can be welded in a single pass and a maximum welding speed that can be achieved in a hybrid laser welding process, despite the high penetration capability of modern lasers.

There were a few studies reporting the investigation of the distribution of consumable elements from filler wires in hybrid laser welds. Zhao et al. (2009) used a nickel-rich wire to investigate its penetration in an 11 mm thick steel. It was shown that the wire mixing was dependent on the direction of the melt flow, which was also found to be dependent on the content of oxygen in the liquid metal and the laser-arc configuration. The inward flow direction around laser keyhole was found to be beneficial for the homogeneity of the welds. In work by Karhu et al. (2013), the transport of a duplex filler wire through 20 mm stainless steel was investigated. The welds exhibited a very steep compositional gradient, which was reflected in the difference in microstructure between the top and bottom part of the welds. In some cases, as low as 10 % of filler wire penetrated to the bottom of the fusion zone in hybrid welds and 4 % in laser welds with cold wire feeding. In a recent work by the same authors (Karhu et al., 2019), only 26–56 % of filler wire was reported to penetrate to the bottom of a 10 mm stainless steel joint in hybrid laser welding and 29–67 % in a laser wire process. In both studies, the penetration of filler wire increased with the gap between welded components. Zhou and Tsai (2009) developed a numerical model to study the interactions between the droplets from the gas metal arc welding (GMAW) and the meltpool in hybrid laser welding. It was shown that mixing of filler wire is controlled by the balance between the solidification rate and the behaviour of liquid metal around the keyhole. The process was also affected by the droplet size and the droplet detachment frequency. In another study, Chen et al. (2020) showed that the laser beam plays a crucial role in enhancing the convective transfer of alloying elements in hybrid welds.

From the modelling investigations of the melt flow, it would be expected that the transport and mixing of filler wire with the parent metal are dependent on the solidification rate and the direction and velocity of the melt flow around the keyhole (Zhou and Tsai, 2009). Usually, there are two competing directions of the melt flow in keyhole laser welding, the downward flow induced by the vaporisation pressure and gravity acting on the meltpool is competing against the upward flow by the frictional force of the escaping vapour gases (Rai et al., 2008). The magnitude of each flow depends on the processing parameters and a joint type, e.g. full or partial penetration welds, welding speed, among others. In addition, the electromagnetic force of the arc source in hybrid welding can induce a significant downward force, particularly at higher currents, as demonstrated by Zhou and Tsai (2007), whilst the solidification time dictates how much time the liquid metal from the molten filler wire and parent metal have before the onset of solidification (Zhou and Tsai, 2009). Hence, the penetration of filler wire and weld homogeneity may change unexpectedly with processing parameters.

There has not been any work reported, where fully homogenous hybrid laser welds in thick sections were achieved. In this work, more practical aspects of the transport and mixing of filler consumables are investigated. X 65 grade pipes with different bevel configurations were welded in 2 G welding position (horizontal position) to determine filler mixing. A filler wire with a signature element was used for welding, and then the concentration of this element in the fusion zone was analysed using energy dispersive spectroscopy (EDS). This enabled us to understand the influence of four major groups of parameters on the weld homogeneity, including laser parameters (power density and beam diameter), GMAW (gas metal arc welding) parameters (current and voltage), hybrid process configuration (laser or arc leading) and bevel design. The study gives a guideline on how to achieve fully homogenous deep penetration laser hybrid welds.

2. Experimental procedure

2.1. Material

The base material used in the experiments was X65 steel in the form of seamless pipes with a wall thickness of 17 mm and an external diameter of 219 mm. The consumable filler used was a duplex stainless steel wire (Metrode ER329 N) with a diameter of 1 mm, containing 22.9 % of chromium and 8.6 % of nickel. The chemical compositions of the base metal and filler are shown in Table 1. Prior to hybrid welding, one end of each pipe section was bevelled, cleaned, and then the pipes were tack welded together to ensure zero-gap conditions. Three different bevels with different root face thickness were used, as shown in Fig. 1.

2.2. Equipment and set-up

A YLR8000 fibre laser manufactured by IPG Photonics was used. The laser delivers an output power of up to 8 kW in CW (continuous wave) mode. A Precitec welding head with an optical magnification of 2, coupled with an optical fibre with a core diameter of 300 μm was used for the beam delivery. The laser head was equipped with a collimator with a focal length of 125 mm and a focusing lens with a focal length of 250 mm, giving the focal point beam diameter of 0.61 mm with a top-hat intensity distribution. In some cases, the focussing lenses were changed to achieve additional optical magnifications of 1.6 and 3.2, which resulted in beam diameters of 500 μm and 1000 μm respectively. In all cases the welds were carried out at the focal point, i.e. the beam was focused on the top surface of the root face.

The laser was combined with an S355 Power Wave Lincoln Electric arc welding system, which was operated in a pulsed gas metal arc welding (P-GMAW) mode. To protect the meltpool from oxidation a BOC Argon Shield Heavy argon mixture with 20 % of CO_2 was used as shielding gas. The gas was supplied through the arc torch at a rate of 17 L/min. The total power input to the material from the process was calculated based on the laser output power, measured using a commercial calorimetric power meter and the instantaneous arc power from voltage and current transients measured by a Yokogawa oscilloscope.

The experimental set-up is shown in Fig. 2. The pipes were mounted on a pipe manipulator and rotated with a set rotational speed, whilst both the laser head and the arc torch mounted to a Fanuc robotic arm had a fixed position for the duration of welding. The torch was equipped with a set of x-y-z manual stages to enable adjustment of its position with respect to the laser beam. The arc torch was inclined by a 30° angle from the radial direction against the travel direction, whilst the laser head was positioned in the radial direction to the pipe rotation. The pipes

Table 1
Chemical composition of base metal and filler wire.

Material	C	Mn	Si	Cr	Cu	Mo	Nb	Ni	Al	V	P
Base	0.06	1.63	0.17	0.25		0.065			0.045	0.06	0.005
Filler	0.01	1.6	0.48	22.9	0.09	3.1		8.6			0.02

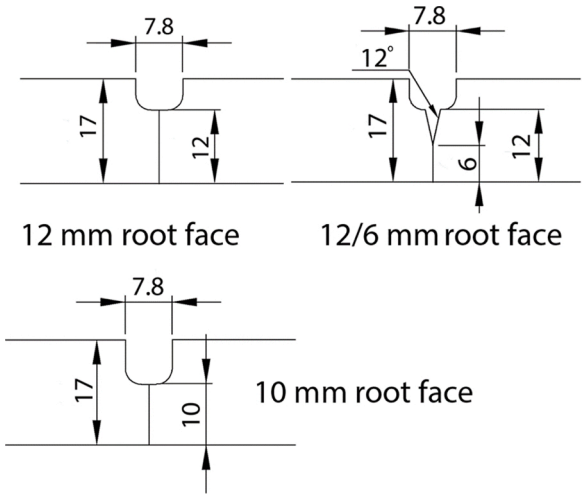

Fig. 1. Bevels used in this study.

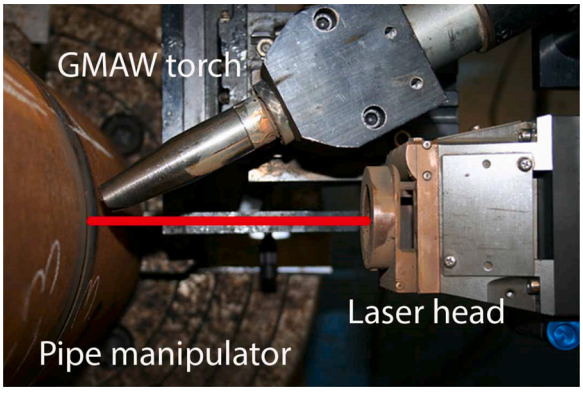

Fig. 2. Experimental set-up as shown from the top.

were welded in 2 G welding position (horizontal welding) with the arc leading welding direction. The 2 G welding position was used to ensure the minimal influence of the gravitational force on the weld profile. As 2 G position is less sensitive to root sagging, this enabled us to study a wider range of processing parameters on weld homogeneity. A separation distance of 2 mm between the laser spot and the tip of the wire in GMAW torch was used as standard, unless otherwise stated, as explained in Section 3.4. All welds presented in this manuscript were carried out at a constant welding speed of 1 m/min.

2.3. Methodology

2.3.1. Wire feed speed (WFS)

Different experimental conditions were tested in order to understand the influence of various processing parameters on the transport and dilution of filler metal. In the first experiment, the effect of wire feed speed was investigated using a bevel with 12 mm root face. The wire feed speed was varied at constant laser conditions to ensure different deposition rates but at constant penetration depth and weld profile. However, because in GMAW the arc power needs to be increased along with the wire feed speed, the increased arc power increases the volume of the melted parent metal and hence dilution. To account for that, a wire volume rate (WVR) was used, defined the ratio of the deposited volume of filler wire (V_{Wire}) to the volume of fusion zone (V_{Melt}), as given by:

$$WVR = \frac{V_{Wire}}{V_{Melt}} = \frac{WFS/_{v} \cdot A_{Wire}}{V_{Melt}} \quad (1)$$

The volume of filler wire was calculated from the wire feed speed to travel speed ratio (WFS/v) and the cross-sectional area of the wire (A_{Wire}) used in the experiments, whilst the volume of fusion zone (V_{Melt}) was measured from the macrographs.

2.3.2. Bevel design

Then the bevel with 12 mm root face was compared with the two remaining bevels from Fig. 2. These particular bevels were chosen to enable us to investigate the influence of the root thickness and bevel geometry on the transport of filler wire across the joint and its dilution with the parent metal. The WFS was varied in such a way to achieve the same WVR of 25 % and 30 % respectively, with all three bevels but with different WFSs and power inputs, which was helpful in understanding the importance of the volume of deposited wire, dilution and power input.

2.3.3. Laser and arc energy

Next, the effect of laser and arc energy, as well as the laser beam diameter was investigated. First, the laser power was varied for two different cases of WFSs of 12 m/min and 16 m/min, corresponding to WVR of 27 % and 30 % respectively. This enabled us to investigate if for a particular WVR the excessive laser power and recoil pressure could transport the deposited wire across the joint and improve its homogeneity. Then the laser beam diameter was varied to understand the influence of power density and recoil pressure, but with as little change of the laser power input as possible. In the first case, the beam diameter could be changed from 0.5 mm to 0.61 mm at constant laser power. In the second case when the beam diameter was increased to 1 mm the laser power had to be increased slightly to compensate for the lower power density to maintain complete penetration weld.

The effect of arc power at constant WFS was also investigated. The arc power was changed from 5.4 kW to 7.8 kW at a constant WFS of 12 m/min, by modifying the waveform characteristics. This was achieved by adjusting a parameter known as trim in Lincoln power sources, which allows for a small adjustment of the arc length and total power at constant WFS. The maximum range was limited by the process stability, as too excessive power for a given WFS results in burning of the contact tip and process failure.

2.3.4. Laser-arc configuration

In the final experiment, other parameters unique for the hybrid process were investigated. As all experiments described so far were carried out with the laser leading and arc trailing configuration, the reversed configuration with the arc leading and laser trailing was also investigated. This was achieved by reversing the direction of the pipe rotation from anti-clockwise to clockwise and remaining all the set-up unchanged. Next, the influence of the laser-arc separation distance on the process stability and weld homogeneity was investigated. In all previously described experiments, the relative distance between the intersection of the laser beam with the top surface of the root face and the wire tip was 2 mm, this was used as standard. But in some

experiments the arc-laser separation distance was varied from 0 mm to 8 mm by moving the arc torch with respect to the laser head by adjusting the position of one of the manual x-y-z stages.

2.4. Analysis

Upon completion of welding, the pipes were sectioned, polished and etched with 2 % Nital solution. Since chromium alloys are resistant to nitric acid, which is the main reactive compound in this etchant, it was only reacting with the low carbon steel, whilst leaving the chromium-rich metal unetched. This particular etchant enabled for a clear visual distinction between the chromium-rich metal from the filler wire and the remaining parent metal. The macrographs were analysed under an optical microscope and then using energy dispersive spectroscopy (EDS). To understand the transport and mixing of filler wire in the fusion zone, chromium was used as a signature element, whose distribution was measured from the top to the bottom of each joint by EDS. The measurements were carried out at an interval of 1 mm. Based on all measurement points, an arithmetic average value of chromium in the entire fusion zone was calculated ($Cr\%_{Avg.}$). To quantify the homogeneity of each weld, the standard deviation was calculated based on the relative difference in chromium concentration, measured at equal intervals through the thickness, with respect to the average chromium concentration.

3. Results

3.1. Effect of wire feed speed (WFS)

Fig. 3 shows the results for 12 mm bevel. The WFS, along with the arc power (current) was varied at constant laser parameters. At low WFS, the welds are clearly separated into two zones, the filler wire-rich zone at the top and the parent metal-rich zone further below. The homogeneity of the welds improved with increasing WFS and arc power until a fully homogenous weld was achieved at a WFS of 20 m/min. The surface of the underside profile of each root is also shown in Fig. 3. In all cases, acceptable root profiles were achieved, indicating stable process and well-developed keyhole. The ratio of the deposited filler wire to the total volume of molten metal, referred to as wire volume ratio (WVR), was calculated for each case. It can be seen that even in the best case of WFS of 20 m/min, corresponding to the upper limit of most standard arc power sources, only 30 % of WVR could be achieved. This means that even in the best case, the fusion zone consisted only of 30 % of the filler metal and the remaining 70 % was contributed from the parent metal, which demonstrates the high dilution of filler wire in deep penetration hybrid laser welding. The maximum WVR is determined by the maximum power capability of an arc source and the root thickness. Note that in this case the arc source was operated at the top limit of wire feed speed and current and to increase the WVR further either a bigger power source or a twin wire process would need to be used or the root thickness reduced.

The results are supported by the measurements of the concentration of chromium using EDS, shown in Fig. 4. Horizontal dashed lines indicate the average concentrations of chromium in each joint. Also, the standard deviations (σ), which characterise the homogeneity of the joints are indicated. The average concentration of chromium increased steadily with increasing WFS, but its distribution did not change much initially, and then improved rapidly when WFS reached 20 m/min. In all cases, apart from the last (WFS of 20 m/min), a steep compositional gradient between the top surface and the bottom of the bevel is observed. High standard deviations indicate the non-uniform composition of the fusion zones. Only in the last case, a low standard deviation of 0.5 was achieved. Note that the concentration of chromium in the filler wire was 22.9 %; however, due to the dilution of the filler by the parent metal, the average measured values are much lower than this.

3.2. Effect of bevel design

In Fig. 5, results for a 12/6 mm bevel are shown. It was expected that with this bevel it would be easier to achieve homogeneous welds, as compared to the standard 12 mm bevel, due to the opening in the root face. At a WFS of 12 m/min quite inhomogeneous joint was achieved, and only when the WFS has increased to 16 m/min the joint homogeneity improved to an acceptable level. Comparing this case to the previous bevel (12 mm), the 12/6 mm bevel required lower WFS to achieve a fully homogenous joint. It is interesting to note that the WFS of 16 m/min resulted in the same WVR of 30 % in the 12/6 mm bevel as the WFS of 20 m/min in the 12 mm bevel. The EDS measurements shown in Fig. 6 confirm that the WFS of 16 m/min was sufficient to achieve a fully homogenous weld. This confirms that the 12/6 mm bevel is easier to penetrate and requires less filler wire than the 12 mm bevel; however, both bevels required at least 30 % of WVR to achieve fully homogenous

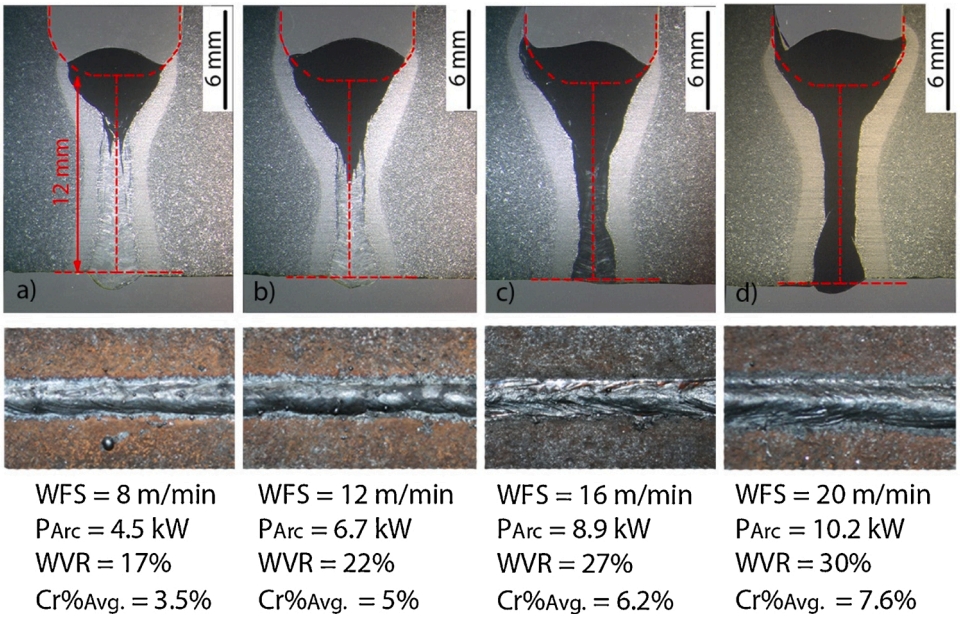

Fig. 3. Effect of wire feed speed and arc energy on penetration of filler wire and root profile in 12 mm bevel; laser power of 8 kW and beam diameter of 0.61 mm.

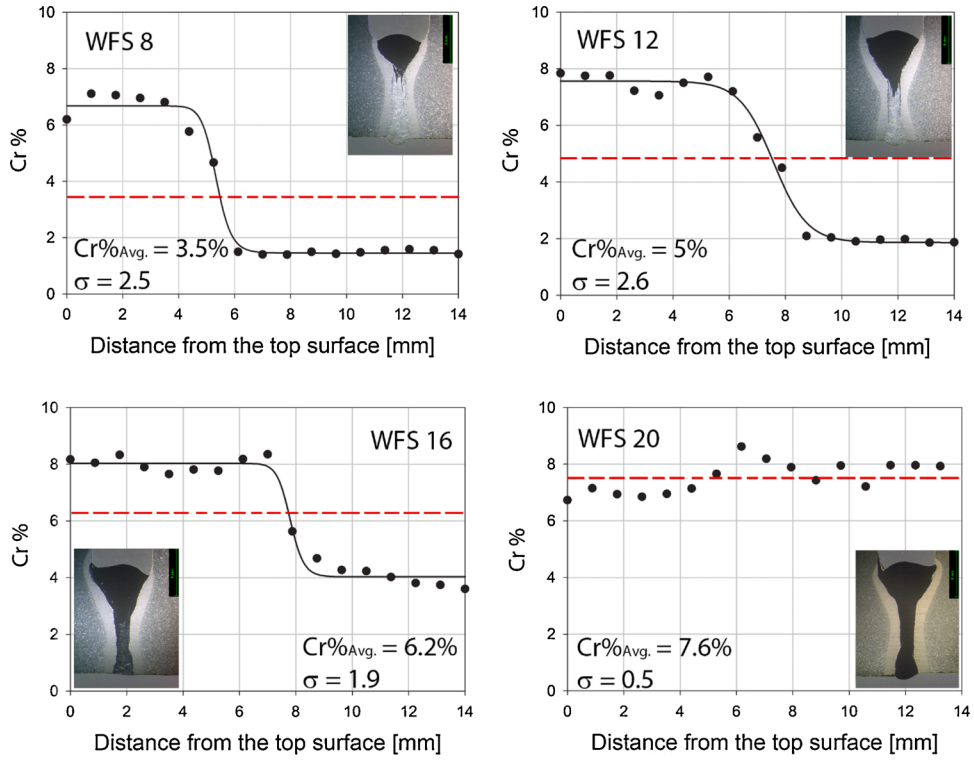

Fig. 4. Distribution of chromium across thickness in welds from Fig. 3.

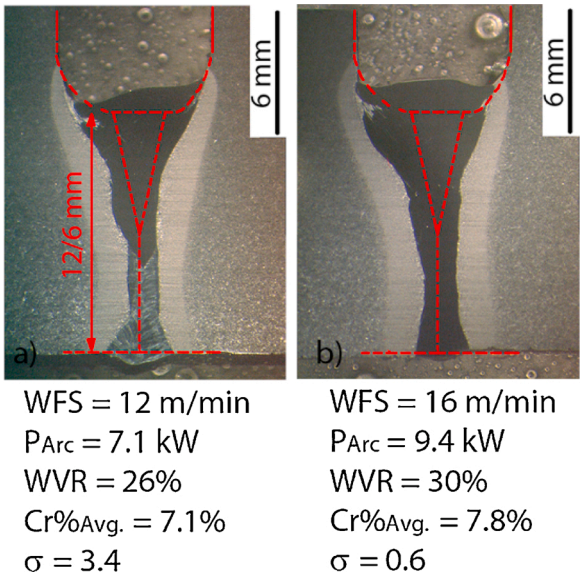

Fig. 5. Effect of wire feed speed on penetration of filler wire in 12/6 mm bevel; laser power of 6 kW and beam diameter of 0.61 mm.

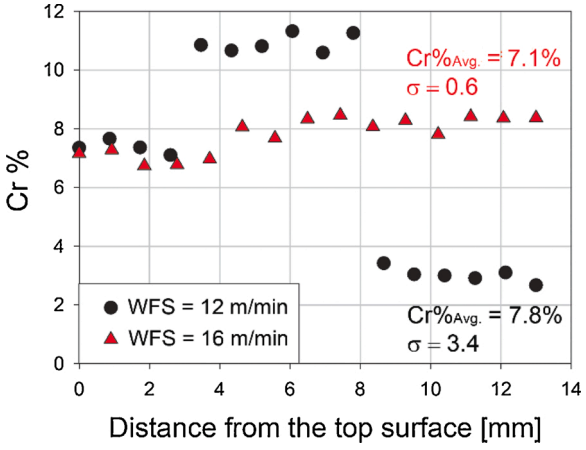

Fig. 6. Distribution of chromium across thickness in welds from Fig. 5.

joints.

It is interesting to notice in Fig. 5 that for a lower WFS of 12 m/min, below the optimum threshold for good homogeneity, a significant proportion of the filler wire was accumulated at a half thickness, exactly at the location of the opening in the root face. This could be attributed to a complex melt flow exacerbated by the small opening in the bevel.

In Fig. 7, similar results for a 10 mm bevel are shown. In this case, the WFS of 16 m/min also resulted in a fully homogenous joint. The concertation distribution plots in Fig. 8 confirm this. Similarly, as in the 12/6 mm bevel, here also the WFS of 16 m/min resulted in a WVR of 30 % and a fully homogenous weld. Note that the laser power was different to compensate for the different root thickness. It is also interesting to notice that both welds exhibit similar reinforcements, despite using different WFS and the same travel speed. Some extra filler metal was used to form the bottom of the root and also it is likely that a proportion of it was lost through spatter on the underside.

3.3. Effect of laser and arc energy

Fig. 9 shows two welds in a 10 mm bevel achieved with different laser powers. Both macrographs exhibit fairly homogenous welds with almost the same average chromium content, the second weld with a marginally lower average chromium content. This is caused by a greater volume of parent metal being melted and diluting the filler wire due to the higher laser power. However, the standard deviation indicates a much higher compositional gradient in the first weld. The weld in Fig. 9a, exhibits a distinguishable deficiency of chromium in the lower

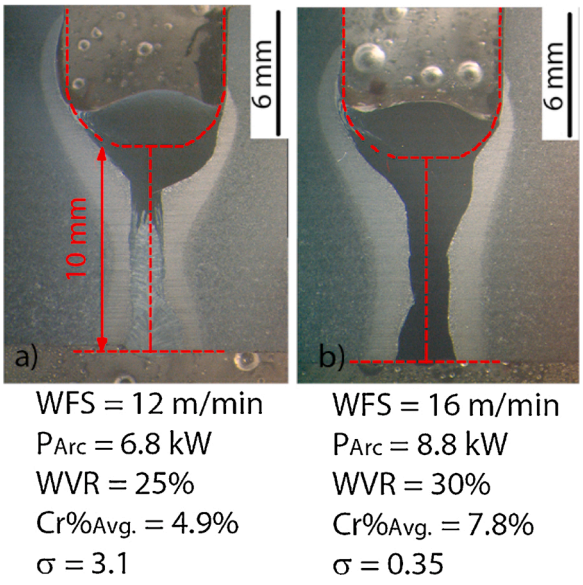

Fig. 7. Effect of wire feed speed on penetration of filler wire in 10 mm bevel; laser power of 7 kW and beam diameter of 0.61 mm.

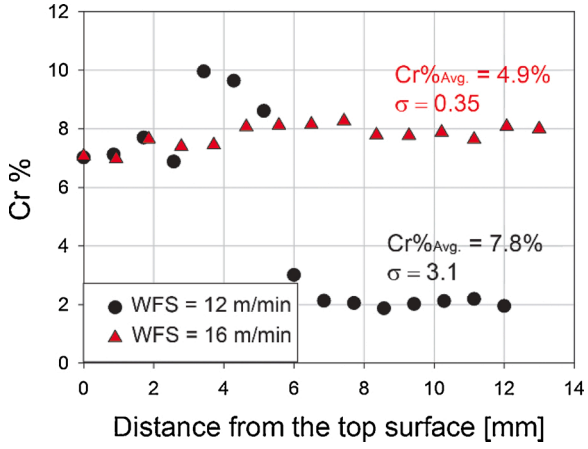

Fig. 8. Distribution of chromium across thickness in welds from Fig. 7.

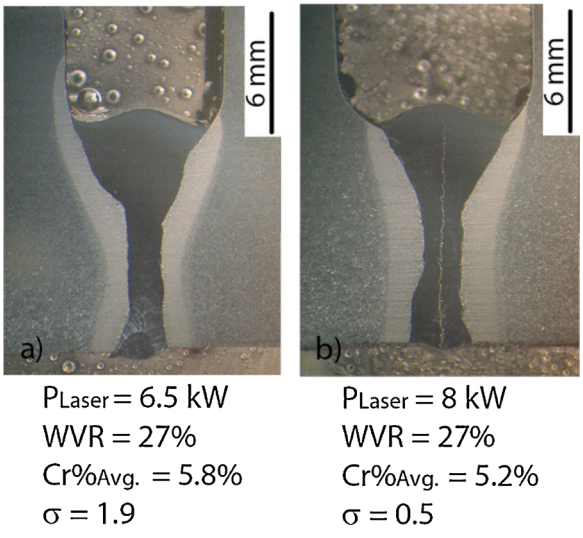

Fig. 9. Effect of laser power on penetration of filler wire in 10 mm bevel; WFS of 12 m/min and beam diameter of 0.61 mm.

part of the bevel, which is also confirmed in Fig. 10. It should be pointed out, that a minimum laser power required for full penetration in this bevel was 6 kW; however, for better consistency of the root, a minimum of 6.5 kW was used. When the laser power was increased to 8 kW in Fig. 9b, the weld profile changed noticeably, the weld broadened in the middle and bottom regions of the root face, and the standard deviation decreased from 1.9 to 0.5, indicating a more uniform distribution of chromium. The average concentration of chromium did not change, which indicates that the increased laser power resulted in redistributing the same volume of filler metal more uniformly across the thickness, as shown in Fig. 10.

Note that the crack visible in Fig. 9b indicates a homogenous weld composition, which resulted in an increased hardenability and susceptibility to cracking. It should be pointed out, that this filler wire, having a high content of chromium, was used purely due to its excellent traceability in the fusion zone; however, this wire is not acceptable for structural welds in this type of steels.

In Fig. 11, the same effect of changing the laser power, but at higher wire feed speed (16 m/min) and higher arc power is shown. It can be seen that here the same increase of laser power did not have any significance on the wire penetration. In both cases, even with the lower laser power, fully homogenous welds were achieved.

In Fig. 12, the effect of laser beam diameter on the homogeneity of hybrid welds is shown. Three different cases are compared. In the first case (Fig. 12a) a beam diameter of 0.5 mm was used, which is smaller than the standard beam of 0.61 mm used in all the results presented so far, for comparison shown in Fig. 12b. The reduction of beam diameter and the associated with it increase in power density improved the transport and mixing of filler wire, which is reflected by the improvement of the standard deviation from 3.1 to 1.05. In the last case (Fig. 12c) the beam diameter was increased to 1 mm, and the laser power was increased to 8 kW, in order to compensate for lower power density. It can be seen that the filler wire mixing improved even further, despite the lowest power density in this case. The highest power density of 3.6 M/Wcm^2 was achieved in the first case, followed by 2.4 MW/cm^2 in the second case and 1 MW/cm^2 in the third case. This indicates that besides power density, the total applied energy and its effect on the viscosity and solidification rate are also important in the transport and mixing of filler wire.

In Fig. 13, the energy input of the arc source was changed, whilst maintaining the same WFS. This was achieved by changing the waveform characteristics of the power source, which allowed for a change in current and voltage at a constant WFS. Despite increasing the arc power from 5.4 kW to 7.8 kW, the weld homogeneity did not change in Fig. 13. Actually, both the WVR and the standard deviation increased with the arc power. This suggests that the higher arc energy was mainly utilised for melting of the parent metal, which resulted in a higher dilution of

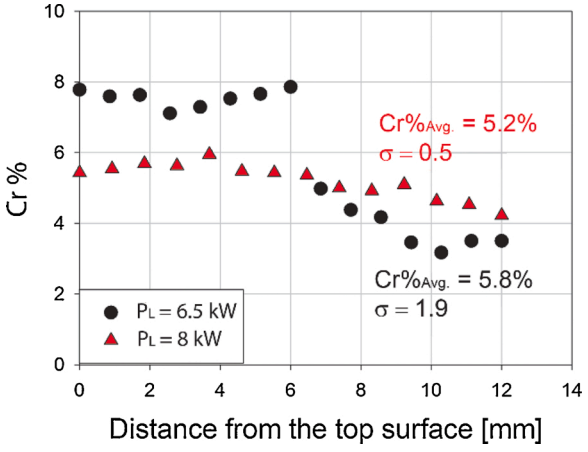

Fig. 10. Distribution of chromium across thickness in welds from Fig. 9.

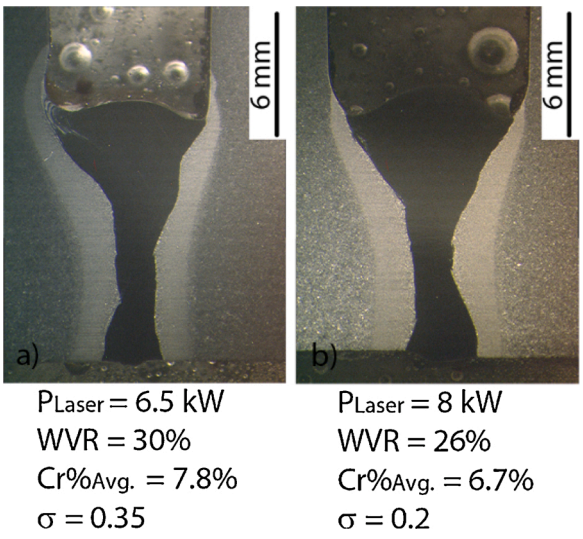

Fig. 11. Effect of laser power on penetration of filler wire in 10 mm bevel; WFS of 16 m/min and beam diameter of 0.61 mm.

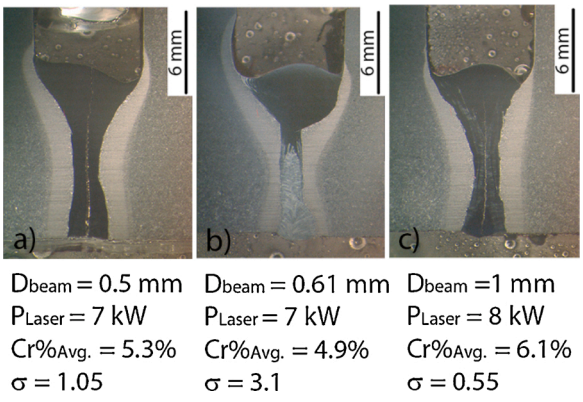

Fig. 12. Effect of laser power and beam diameter on penetration of filler wire in 10 mm bevel; WFS of 12 m/min.

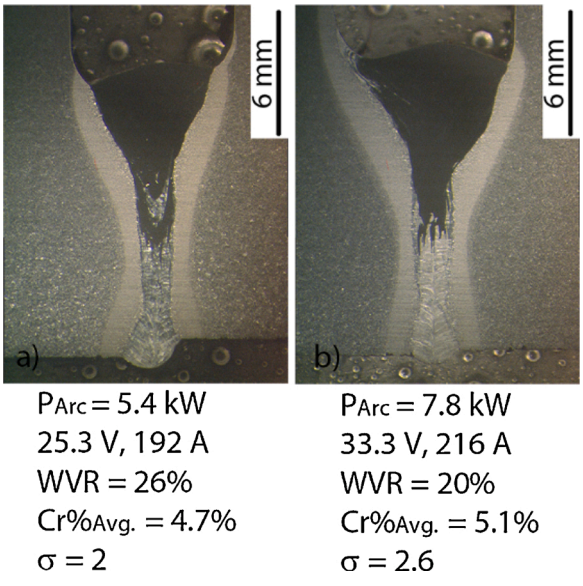

Fig. 13. Effect of arc power on penetration of filler wire in 12 mm bevel; WFS of 12 m/min, laser power of 8 kW and beam diameter of 0.61 mm.

filler wire without any effect on its penetration.

3.4. Laser-arc configuration

In the final experiment, the effect of additional parameters of hybrid laser welding was investigated. In Fig. 14, the laser leading configuration was compared with the arc leading configurations for the same processing parameters. The laser leading case resulted in a marginally better transport of the filler wire with a lower convexity of the weld profile, which is more desirable.

The laser-arc separation distance is another parameter that is inherently associated with the hybrid welding. As shown in Fig. 15, up to a distance of 6 mm between the tip of the wire and the laser spot, there is no significant difference in the homogeneity of the welds. Only when the separation distance increased to 8 mm, the hybrid process collapsed, and the weld profile converted into a partially penetrated joint. It should be noted, that at zero-separation distance, the arc characteristics exhibited slightly more instabilities and spatter than with any other case, attributed to the interactions between the droplets and the laser-generated meltpool, which disturbed the arc. However, the data in Fig. 15 demonstrate a relatively high tolerance of the hybrid laser welding to the separation distance.

4. Discussion

4.1. WFS and bevel shape

Deep penetration hybrid laser welds are susceptible to inhomogeneous composition due to the deficiency of filler wire and a high volume of molten parent metal. Unlike in multi-pass welding where a bevel is gradually filled up with a filler wire until the complete joint is achieved, in a single-pass hybrid welding the heat source penetrates much thicker root face in one pass. This provides a large amount of molten parent metal, which dilutes the filler metal. Hence, even at relatively high deposition rates, a maximum WVR that could be achieved was only 30 %.

For a given material thickness, there is a minimum wire deposition rate required to achieve a particular concentration of filler material in the fusion zone and a minimum energy required to ensure homogenous composition throughout the joint. An obvious way of improving the weld homogeneity is by increasing the WFS along with the arc power, as shown in Fig. 4, which provides a higher concentration of alloying elements and more heat. This extra energy of the arc source does not

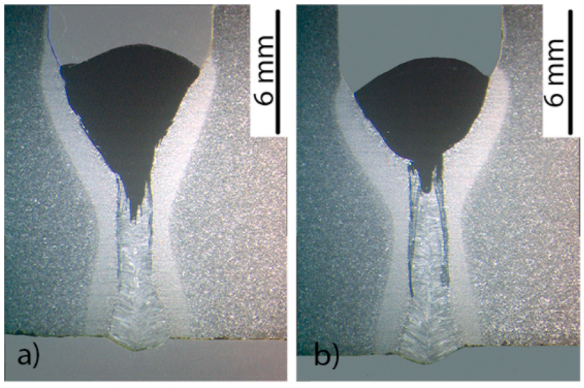

Fig. 14. Effect of leading source on penetration of filler wire in 12 mm bevel; WFS of 12 m/min, laser power of 8 kW and beam diameter of 0.61 mm.

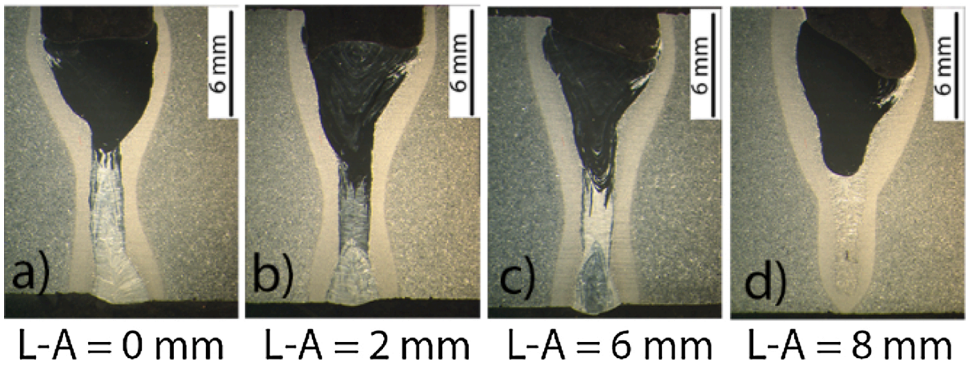

Fig. 15. Effect of laser-arc separation distance on penetration of filler wire in 12 mm bevel; WFS of 12 m/min, laser power of 8 kW and beam diameter of 0.61 mm.

contribute greatly to the penetration depth, since the laser beam provides the main penetrating force; therefore all the welds are fully penetrated, but the extra arc energy can be used to increase the temperature of the meltpool and delay the onset of solidification. The transport of filler wire and joint homogeneity is dependent on the volume of deposited wire, melt velocity and solidification rate (Zhou and Tsai, 2009). It was shown in previous studies, that the molten filler metal from the arc source flows towards the laser-generated keyhole, where it is subsumed and transported inside the keyhole (Li et al., 2020). Higher WFS means more filler metal in the meltpool, which should increase the concentration of filler elements in the weld metal, however, to ensure a fully homogenous weld, the liquid metal has to have enough time to reach the bottom of the root. Hence, higher arc energy increases this likelihood by lowering the temperature-dependent viscosity of the metal and by delaying the solidification.

Using different bevels with different root faces and shapes enabled us to investigate if the WVR or the heat input is more important in the weld homogeneity. A standard 12 mm bevel (Fig. 4) should require a higher WFS and more power to achieve a fully homogenous weld, than a two-step 12/6 mm bevel (Fig. 6), which was the case. The opening in the root face in the 12/6 mm bevel reduced both, the thickness needed to be penetrated by the laser and the dilution of the filler metal. However, when comparing the 12/6 mm bevel with a standard 10 mm bevel, the benefit was not that great, the former requiring just less laser power to achieve the full penetration.

When comparing all three bevels near-threshold conditions for full homogeneity, the 12/6 mm bevel imposed the lowest resistance for the filler wire to be transported to the bottom of the joint, followed by 10 mm and 12 mm bevels. Nevertheless, all three bevels required a minimum of 30 % of WVR to achieve fully homogenous welds, but each case needed different WFS to satisfy this threshold WVR. In Fig. 16, all three bevels are compared in terms of the power required to melt a particular volume of metal. It can be seen that the same amount of energy per unit volume of melted material was required in all the joints. This suggests that the process is self-balanced, meaning that even if different bevels require different wire deposition rates to achieve a particular constituent composition, the energy required to ensure the complete fusion is fixed.

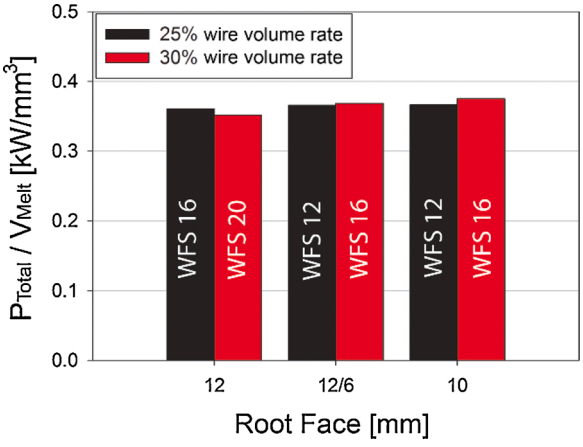

Fig. 16. Ratio of applied power of laser and arc to the melt volume as a function of root face thickness.

The data presented in this work indicate that the transport of filler wire does not respond linearly to the welding parameters. A small change in processing parameters at the initial stage may not have any effect on the joint homogeneity, and only after a certain point, the filler metal starts being transported to the bottom of the joint and mixed properly. This is additionally exacerbated by the bevel shape. Considering just the thickness of the material, the 12/6 mm bevel should be the most likely to achieve fully homogenous welds from all tested bevels, however, the accumulation of the filler detected at a half thickness for a WFS of 12 m/min in Fig. 6, indicates some complex melt flow behaviour. This is consistent with previous studies by Mazar Atabaki et al. (2014), who showed that V-grooves are more susceptible to oscillations and perturbation of the liquid metal than grooves with a shoulder. It is known from numerical modelling that the downward momentum of the filler droplets, in partially penetrated welds is eventually transformed into an outward flow at the bottom of the keyhole, which results in a vortex (Zhou and Tsai, 2009). Such a vortex can be additionally enhanced by the frictional force of vapour gases escaping from a keyhole, as demonstrated by Fabbro et al. (2004). A similar vortex could be induced at the bottom of the V-groove in the 12/6 mm bevel. Therefore, at low energy conditions, the wire did not penetrate to the bottom of the root as efficiently as it was expected, despite the lower effective root face thickness.

4.2. Laser and arc energy

The transport of filler wire across the thickness can also be improved by increasing the energy or power density of the laser beam. Homogeneity of the hybrid laser welds was significantly improved by increasing the laser power in Fig. 10. Similarly, the homogeneity was improved by increasing the power density at constant laser power, by reducing the laser spot diameter (Fig. 12). However, the effect was not as significant as in the case of changing the laser power.

The effect of improved weld homogeneity with increased laser power or reduced beam diameter is attributed to the increased power density and vaporisation pressure. The recoil pressure, which is responsible for the generation of keyhole provides the downward velocity to the liquid metal inside the keyhole (Eriksson et al., 2011). The absorbed laser energy induces local high pressure zones on the front wall of the keyhole, which drives the molten metal down to the bottom of the keyhole. The higher the downward velocity, the higher the chance for the molten filler metal to reach the bottom of a joint. It was shown in

previous studies that a quite significant mass transfer is required for the liquid to be transported by the thin melt film on the keyhole walls before the solidification takes place (Eriksson et al., 2013). Hence, the power density has a significant effect on the transport and mixing of filler wire and hence weld homogeneity.

In addition to the downward velocity, also the solidification time and temperature of the liquid are important (Zhou and Tsai, 2009). The longer the solidification time and the lower the viscosity of the liquid, which is inversely proportional to the temperature, the higher the likelihood of achieving fully homogenous joints. Thus, the laser power had a greater effect on the transport and mixing of wire than the beam diameter in Fig. 12, because it increases both, the vapour pressure and temperature of the liquid, which increases the downward velocity of the liquid and delays the solidification.

The energy input of hybrid laser welding can also be varied by changing the arc power. In most GMAW processes, the arc current and power is automatically adjusted by the feedback control system according to the selected WFS. However, a small adjustment of the arc power at constant WFS is possible by changing the waveform parameters. In an example in Fig. 13, the arc power was increased from 5.4 kW to 7.8 kW, but the weld homogeneity did not improve, even worsened. Any change in the arc power at constant WFS in GMAW process affects mainly the burn-off rate and arc length. The increased arc length resulted in a broadening of the arc plasma, which then melted the sidewalls of the bevel more extensively, providing more liquid parent metal. Hence, dilution of the filler wire increased, having little effect on its transport across the joint. Therefore, the weld homogeneity can only be improved by increasing the arc current, as in the case of increasing WFS (Fig. 4).

In Fig. 17, both the effects, the increase of the arc power by changing the arc current (WFS) and the voltage (arc length), are compared. It can be seen, that the weld homogeneity, indicated by the ratio of chromium concentration at the bottom of a joint to the average chromium concertation in the whole joint, increases exponentially with current and is independent of the voltage. The data indicate that there is a threshold current, above which the homogeneity improves rapidly. This is attributed to the electromagnetic force and its quadratic dependence with the current. The liquid droplets of the filler wire, accelerated within this electromagnetic field, can transfer significant kinetic energy to the workpiece, inducing a high pressure on the liquid metal, as shown by Gao et al. (2008). Therefore, the effect of the current is greater than the effect of voltage. However, it should be pointed out, that controlling the transport and mixing of the filler wire by the arc current is more complex and less reliable, than controlling it by the laser power.

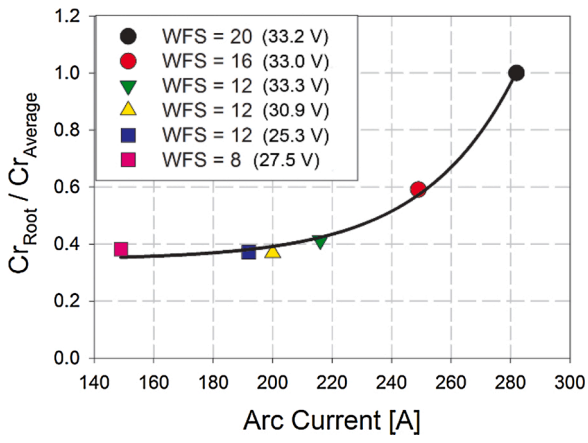

Fig. 17. Effect of arc current on weld homogeneity (ratio of chromium at the bottom of the root to the total average deposited) in 12 mm bevel joint; laser power 8 kW and beam diameter of 0.61 mm.

4.3. Process configuration

In the final experiment, the effect of additional parameters, such as the leading source and the separation distance, were investigated. The laser leading resulted in a marginally better weld homogeneity than the arc leading configuration (Fig. 14), which is in agreement with the findings of Zhao et al. (2009) and Liu et al. (2012). However small, but the difference is attributed to the melt flow direction around the keyhole, as shown schematically in Fig. 18. When the arc torch is pushing behind the laser, in the laser leading configuration, the velocity vector of the filler metal acts in the opposite direction to the welding speed-induced melt flow. This forces the filler metal flow to slow down and reverse its direction, which induces a vortex behind the keyhole. As a result, the filler metal stays longer in the vicinity of the laser interaction zone and has a better chance to be transported by the laser recoil pressure to the bottom of the keyhole. In contrast, in the arc leading configuration, the filler metal flows in the same direction as the liquid metal behind the keyhole, and hence inducing the outward flow. However, the difference in weld homogeneity in Fig. 14 is very low, which indicates that in fully penetrated welds this effect is not very significant. The main benefit of the laser leading seems to be a flatter top bead profile, which is desired in most welding applications.

The laser-arc separation distance is another parameter that is inherently associated with the hybrid welding. In theory, increasing this distance should decrease the efficiency of the process and lead to less effective transport of the filler wire across the joint. However, the results shown in Fig. 15 indicate that the process is very tolerant to the separation distance, which is attributed to the size of the meltpool and the melt flow direction.

4.4. Parameters controlling wire penetration

It has been shown in previous paragraphs that the transport and mixing of the filler wire is dependent on the WFS, laser power, laser spot diameter, arc power, leading source and root thickness. In principle, there are two aspects to be controlled, one is the average content of an alloying element in the meltpool, and another is the weld homogeneity. The former being dependent on the content of a particular element in the wire and its dilution with the parent metal, whilst the fusion zone homogeneity for a particular root thickness should be dependent primarily on the power density of the heat source.

The average deposited content of a filler element (Nx_{AvgDep}), chromium in this case, in the fusion zone should be directly proportional to the product of the deposited volume of filler wire (V_{Wire}) and concentration of this element in the wire (Nx_{Wire}), and inversely proportional to the volume of fusion zone (V_{Melt}), as given by the following equation.

$$Nx_{AvgDep} \approx \frac{V_{Wire} \cdot Nx_{Wire}}{V_{Melt}} [\%] \tag{2}$$

The volume of deposited filler wire is given by:

$$V_{Wire} = \frac{WFS}{v} A_{Wire} [m^3] \tag{3}$$

where WFS/v is the wire feed speed to travel speed ratio, and A_{Wire} is the cross-sectional area of the wire. The volume of the combined liquid metal from filler wire and parent metal (V_{Melt}) should be proportional to the combined heat input (HI), which is given by:

$$V_{Melt} \approx HI = \frac{aP_L + bP_A}{v} \left[m^3\right] \tag{4}$$

where a and b are heat transfer coefficients for laser and arc respectively, P_L is laser output power, P_A is arc power, and v is the welding speed. Substituting Eqs. 3 and 4 into Eq. 2 gives,

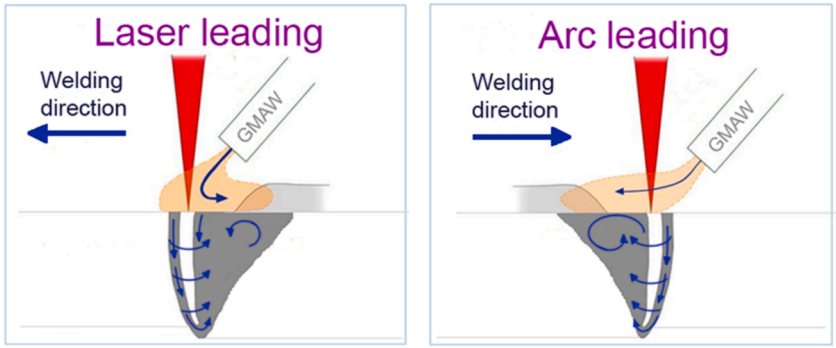

Fig. 18. Schematic of melt flow direction in laser leading and arc leading.

$$Nx_{AvgDep} \approx \frac{WFS \cdot A_{Wire} \cdot Nx_{Wire}}{aP_L + bP_A}\left[\%\right] \quad (5)$$

The real measured average chromium distribution plotted as a function of Eq. 5, is shown in Fig. 19. The average concentration of chromium is directly proportional to the product of the wire deposited and the average content of chromium within the wire and inversely proportional to the combined power input. Note that heat transfer coefficients for both heat sources were assumed to be unity.

The appropriate concentration of a filler element in the fusion zone does not necessarily mean a homogenous weld, because the filler can be concentrated within a particular region of the fusion zone. In order to spread the deposited amount of wire across the entire thickness and achieve a homogenous weld, a certain penetrating force is also required. The concentration of a particular filler element in the root (Nx_{Root}), should be directly proportional to the product of combined laser and arc power density (q), interaction time (t_i), average deposited content of the filler element (Nx_{AvgDep}) in the entire fusion zone, and inversely proportional to the root thickness (L). If we assume a simplified power density, as being the ratio of combined laser and arc power (aP_L+bP_A) to the laser spot diameter (d_L), and the interaction time as being the ratio of welding speed to the laser spot diameter, the concentration of a filler element in the root is given by:

$$Nx_{Root} \approx q \cdot t_i \cdot \frac{1}{L} \cdot Nx_{AvgDep} \approx \frac{aP_L + bP_A}{d_L} \cdot \frac{d_L}{v} \cdot \frac{1}{L} \cdot Nx_{AvgDep}\left[\%\right] \quad (6)$$

We can rearrange Eq. 6 to achieve the concentration of a particular filler element in the root normalised by the average deposited content of this element in the entire weld, which is helpful in characterising the homogeneity of welds, as given by:

$$\frac{Nx_{Root}}{Nx_{AvgDep}} \approx \frac{aP_L + bP_A}{Lv} \quad (7)$$

In Fig. 20, the normalised concentration of chromium in the root of all welds from this work plotted as a function of Eq. 7 is shown. It can be seen, that at a low level of process energy there is a big difference between the amount of chromium in the root and the average chromium content in the meltpool, despite all of them being full penetration welds. Only at a certain energy level, fully homogenous fusion zones could be achieved.

Some processing parameters play contradicting roles between the average chemistry of the fusion zone and its homogeneity. The laser power and arc power are one of the examples. Both of them can improve the weld homogeneity, and at the same time, they contribute to the increased dilution of the filler wire by melting more parent metal. Since the arc will melt the parent metal in a greater extent than the laser, it is recommended to use the arc primarily for melting of the consumable to ensure the right weld chemistry, and then control the transport of the wire across the joint by the laser source. However, it is anticipated that the right balance between the applied energy and the wire deposition will become more and more challenging as the joint thickness increases, until a point when the complete fusion with full homogeneity is not possible anymore. At this point, a multi-pass strategy should be used. It should also be pointed out, that in all conditions presented in this paper all bevels were set-up with a zero-gap configuration; however, even a small gap in the fit-up should improve the filler wire penetration.

The presented data indicate that in the case of structural welds, whose quality requirements stipulate the use of appropriate filler consumables for the control of microstructure and properties, the maximum joint thickness that can be welded in a single pass is not limited by the maximum output power of available lasers, but rather by the weld

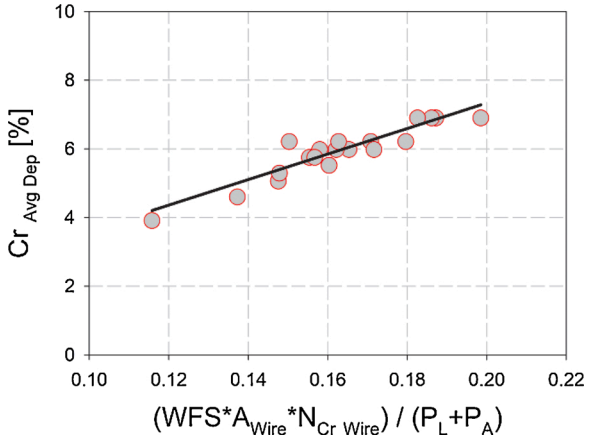

Fig. 19. Average measured chromium content in the meltpool as a function of the ratio of wire deposition to the power input (Eq. 5).

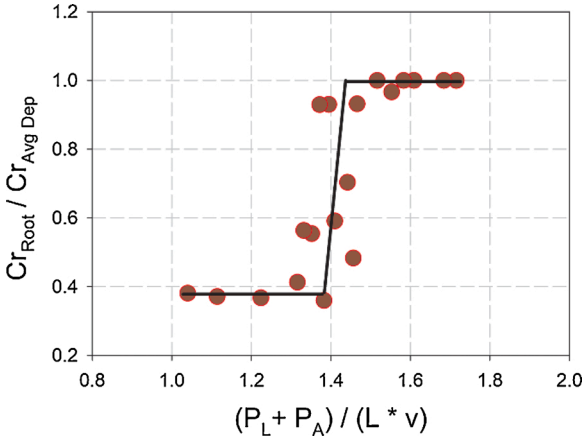

Fig. 20. Relative concentration of chromium in the root to the total deposited chromium as a function of Eq. 7.

homogeneity. The weld homogeneity is limited by the maximum wire volume that can be deposited reliably by the arc source and transported by the laser beam across the entire thickness. Hence, in reality, the material thickness or the root thickness in a multi-pass approach has to be reduced to ensure a fully homogenous joint with required composition, despite enormous power availability of modern lasers. Furthermore, the driving forces of the filler and the response of weld homogeneity to the processing parameters is envisaged to be the same for different welding positions, i.e. 1 G, 2 G etc. However, it should be pointed out that in 1 G position (vertical torch) the process tolerance to sagging is lower than in 2 G (horizontal torch), and in some cases, the power density of the laser will have to be limited to stay below the root sagging threshold for a given joint thickness and gap. This means that the user may need to trade-off the weld homogeneity with sagging, and this may limit the productivity further.

5. Conclusions

Transport of filler wire across the joint and its mixing with the parent metal in hybrid laser welds was studied in this work. Various bevels and many experimental conditions were tested. It can be concluded, that the most important aspects in the penetration of filler wire are, the proportion of deposited wire to the total volume of fusion zone, and the sufficient penetration force to transport it across the joint. In general, in hybrid laser welds, a significant volume of molten parent metal is present in the fusion zone, due to the relatively high thickness of the material being welded in one pass. This liquid parent metal dilutes the deposited filler wire, contributing to a lean chemical composition of the fusion zone. The maximum wire volume rate achieved in this study was in the order of 30 %. The best way of improving the homogeneity of the hybrid welds is to increase the laser power and arc current. The effect of the laser beam diameter is more complex. The challenge of achieving fully homogenous welds increases with increasing the material thickness. The transport of filler wire and weld homogeneity can be one of the mains factors limiting the maximum joint thickness that can be welded in a single pass using hybrid laser welding process.

Data statement

Data underlying this study can be accessed through the Cranfield University repository at https://doi.org/10.17862/cranfield.rd.13547420.v1.

CRediT authorship contribution statement

W. Suder: Conceptualization, Funding acquisition, Methodology, Investigation, Writing - original draft, Visualization. **S. Ganguly:** Conceptualization, Methodology, Funding acquisition, Writing - review & editing. **S. Williams:** Conceptualization, Resources, Funding acquisition, Writing - review & editing. **B.Y.B. Yudodibroto:** Supervision, Resources, Writing - review & editing.

Declaration of Competing Interest

The authors declare that they have no known competing financial interests or personal relationships that could have appeared to influence the work reported in this paper.

Acknowledgements

This research was carried out under project number M31.8.12461 in the framework of the Research Program of the Materials Innovation Institute M2i (www.m2i.nl). Financial support provided by the industrial partner Heerema Marine Contractors(www.hmc.heerema.com) is also acknowledged.

References

Chen, X., Yu, G., He, X., Li, S., Li, Z., 2020. Numerical study of heat transfer and solute distribution in hybrid laser-MIG welding. Int. J. Therm. Sci. https://doi.org/10.1016/j.ijthermalsci.2019.106182.

Courtois, M., Carin, M., Masson, P.Le, Gaied, S., Balabane, M., 2013. A new approach to compute multi-reflections of laser beam in a keyhole for heat transfer and fluid flow modelling in laser welding. J. Phys. D Appl. Phys. https://doi.org/10.1088/0022-3727/46/50/505305.

Eriksson, I., Powell, J., Kaplan, A.F.H., 2011. Measurements of fluid flow on keyhole front during laser welding. Sci. Technol. Weld. Join. https://doi.org/10.1179/1362171811Y.0000000050.

Eriksson, I., Powell, J., Kaplan, A.F.H., 2013. Melt behavior on the keyhole front during high speed laser welding. Opt. Lasers Eng. https://doi.org/10.1016/j.optlaseng.2013.01.008.

Fabbro, R., Hamadou, M., Coste, F., 2004. Metallic vapor ejection effect on melt pool dynamics in deep penetration laser welding. J. Laser Appl. https://doi.org/10.2351/1.1642633.

Gao, M., Zeng, X.Y., Hu, Q.W., Yan, J., 2008. Weld microstructure and shape of laser-arc hybrid welding. Sci. Technol. Weld. Join. https://doi.org/10.1179/174329307X249388.

Hayashi, T., Katayama, S., Abe, N., Omori, A., 2004. High-power CO2 laser-MIG hybrid welding for increased gap tolerance. Hybrid weldability of thick steel plates with a square groove. Weld. Int. https://doi.org/10.1533/wint.2004.3318.

Karhu, M., Kujanpää, V., Gumenyuk, A., Lammers, M., 2013. Study of filler metal mixing and its implication on weld homogeneity of laser-hybrid and laser cold-wire welded thick austenitic stainless steel joints. ICALEO 2013 - 32nd International Congress on Applications of Lasers and Electro-Optics. https://doi.org/10.2351/1.5062883.

Karhu, M., Kujanpää, V., Eskelinen, H., Salminen, A., 2019. Filler metal mixing behaviour of 10 mm thick stainless steel butt-jointwelds produced with laser-arc hybrid and laser cold-wire processes. Appl. Sci. https://doi.org/10.3390/app9081685.

Klein, T., Vicanek, M., Simon, G., 1996. Forced oscillations of the keyhole in penetration laser beam welding. J. Phys. D Appl. Phys. https://doi.org/10.1088/0022-3727/29/2/008.

Kujanpää, V., 2014. Thick-section laser and hybrid welding of austenitic stainless steels. Phys. Procedia. https://doi.org/10.1016/j.phpro.2014.08.056.

Li, F., Tao, W., Peng, G., Qu, J., Li, L., 2020. Behavior and stability of droplet transfer under laser-MIG hybrid welding with synchronized pulse modulations. J. Manuf. Process. https://doi.org/10.1016/j.jmapro.2020.02.017.

Liu, L.M., Yuan, S.T., Li, C.B., 2012. Effect of relative location of laser beam and TIG arc in different hybrid welding modes. Sci. Technol. Weld. Join. https://doi.org/10.1179/1362171812Y.0000000033.

Lu, F., Li, X., Li, Z., Tang, X., Cui, H., 2015. Formation and influence mechanism of keyhole-induced porosity in deep-penetration laser welding based on 3D transient modeling. Int. J. Heat Mass Transf. https://doi.org/10.1016/j.ijheatmasstransfer.2015.07.041.

Mazar Atabaki, M., Ma, J., Yang, G., Kovacevic, R., 2014. Hybrid laser/arc welding of advanced high strength steel in different butt joint configurations. Mater. Des. https://doi.org/10.1016/j.matdes.2014.08.011.

Rai, R., Kelly, S.M., Martukanitz, R.P., DebRoy, T., 2008. A convective heat-transfer model for partial and full penetration keyhole mode laser welding of a structural steel. Metall. Mater. Trans. A Phys. Metall. Mater. Sci. https://doi.org/10.1007/s11661-007-9400-6.

Semak, V., Matsunawa, A., 1997. The role of recoil pressure in energy balance during laser materials processing. J. Phys. D Appl. Phys. https://doi.org/10.1088/0022-3727/30/18/008.

Semak, V.V., Hopkins, J.A., McCay, M.H., McCay, T.D., 1995. Melt pool dynamics during laser welding. J. Phys. D Appl. Phys. https://doi.org/10.1088/0022-3727/28/12/008.

Sokolov, M., Salminen, A., Kuznetsov, M., Tsibulskiy, I., 2011. Laser welding and weld hardness analysis of thick section S355 structural steel. Mater. Des. https://doi.org/10.1016/j.matdes.2011.05.053.

Zhang, M., Chen, G., Zhou, Y., Li, S., 2013. Direct observation of keyhole characteristics in deep penetration laser welding with a 10 kW fiber laser. Opt. Express. https://doi.org/10.1364/oe.21.019997.

Zhang, D., Wang, M., Shu, C., Zhang, Y., Wu, D., Ye, Y., 2019. Dynamic keyhole behavior and keyhole instability in high power fiber laser welding of stainless steel. Opt. Laser Technol. https://doi.org/10.1016/j.optlastec.2019.01.018.

Zhao, L., Sugino, T., Arakane, G., Tsukamoto, S., 2009. Influence of welding parameters on distribution of wire feeding elements in CO2 laser GMA hybrid welding. Sci. Technol. Weld. Join. https://doi.org/10.1179/136217109X434252.

Zhou, J., Tsai, H.L., 2007. Effects of electromagnetic force on melt flow and porosity prevention in pulsed laser keyhole welding. Int. J. Heat Mass Transf. https://doi.org/10.1016/j.ijheatmasstransfer.2006.10.040.

Zhou, J., Tsai, H.L., 2008. Modeling of transport phenomena in hybrid laser-MIG keyhole welding. Int. J. Heat Mass Transf. https://doi.org/10.1016/j.ijheatmasstransfer.2008.02.011.

Zhou, J., Tsai, H.L., 2009. Investigation of mixing and diffusion processes in hybrid spot laser-MIG keyhole welding. J. Phys. D Appl. Phys. https://doi.org/10.1088/0022-3727/42/9/095502.

2021-01-05

Penetration and mixing of filler wire in hybrid laser welding

Suder, Wojciech

Elsevier

Suder W, Ganguly S, Williams S, Yudodibroto BYB. (2021) Penetration and mixing of filler wire in hybrid laser welding. Journal of Materials Processing Technology, Volume 291, May 2021, Article number 117040

https://doi.org/10.1016/j.jmatprotec.2020.117040